Molecular Cell, Volume *58*

Supplemental Information

Autophagic Degradation of the 26S Proteasome Is Mediated by the Dual ATG8/Ubiquitin Receptor RPN10 in *Arabidopsis*

Richard S. Marshall, Faqiang Li, David C. Gemperline, Adam J. Book, and Richard D. Vierstra

Figure S1. Marshall *et al.*

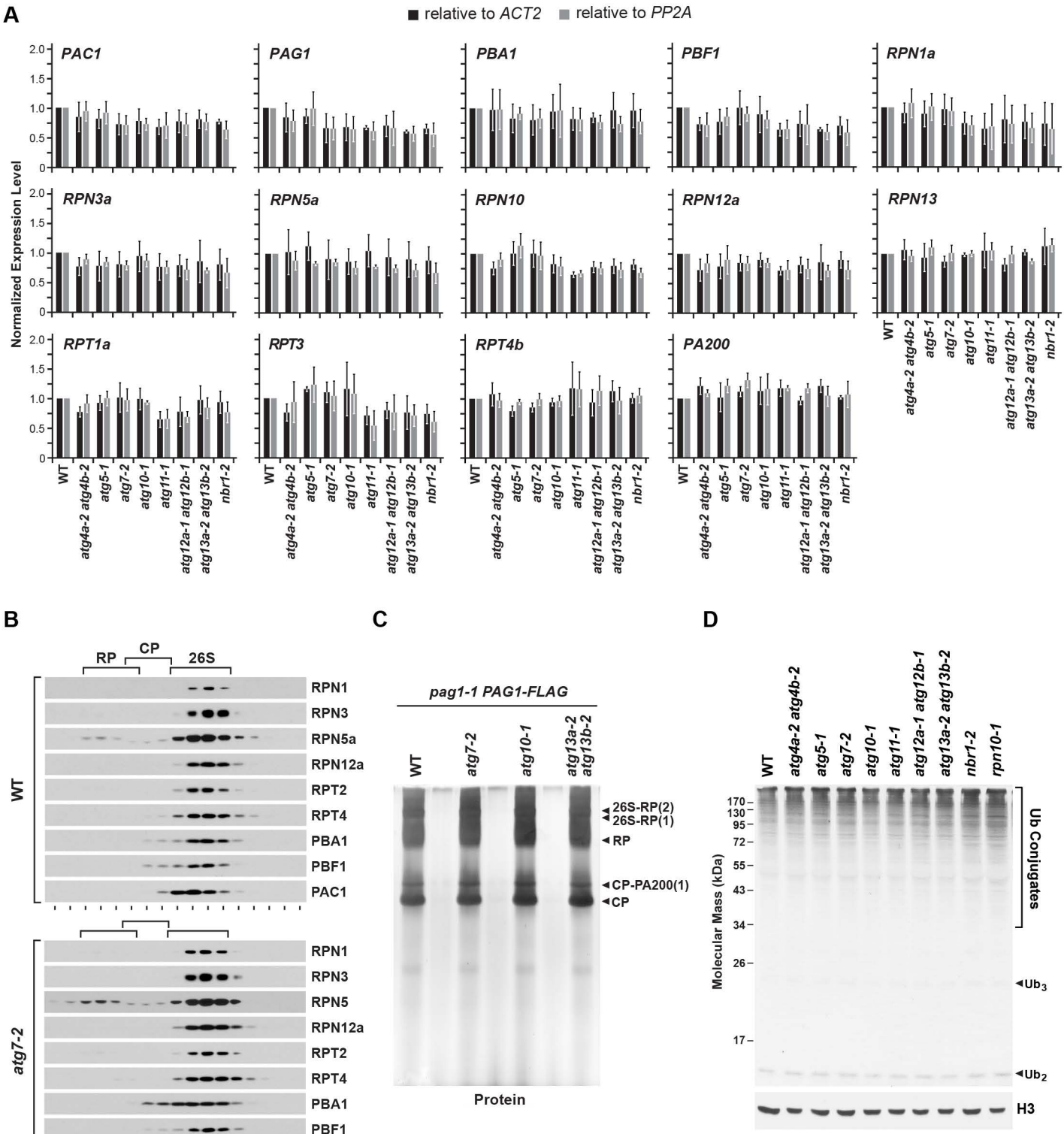

Figure S2. Marshall *et al.*

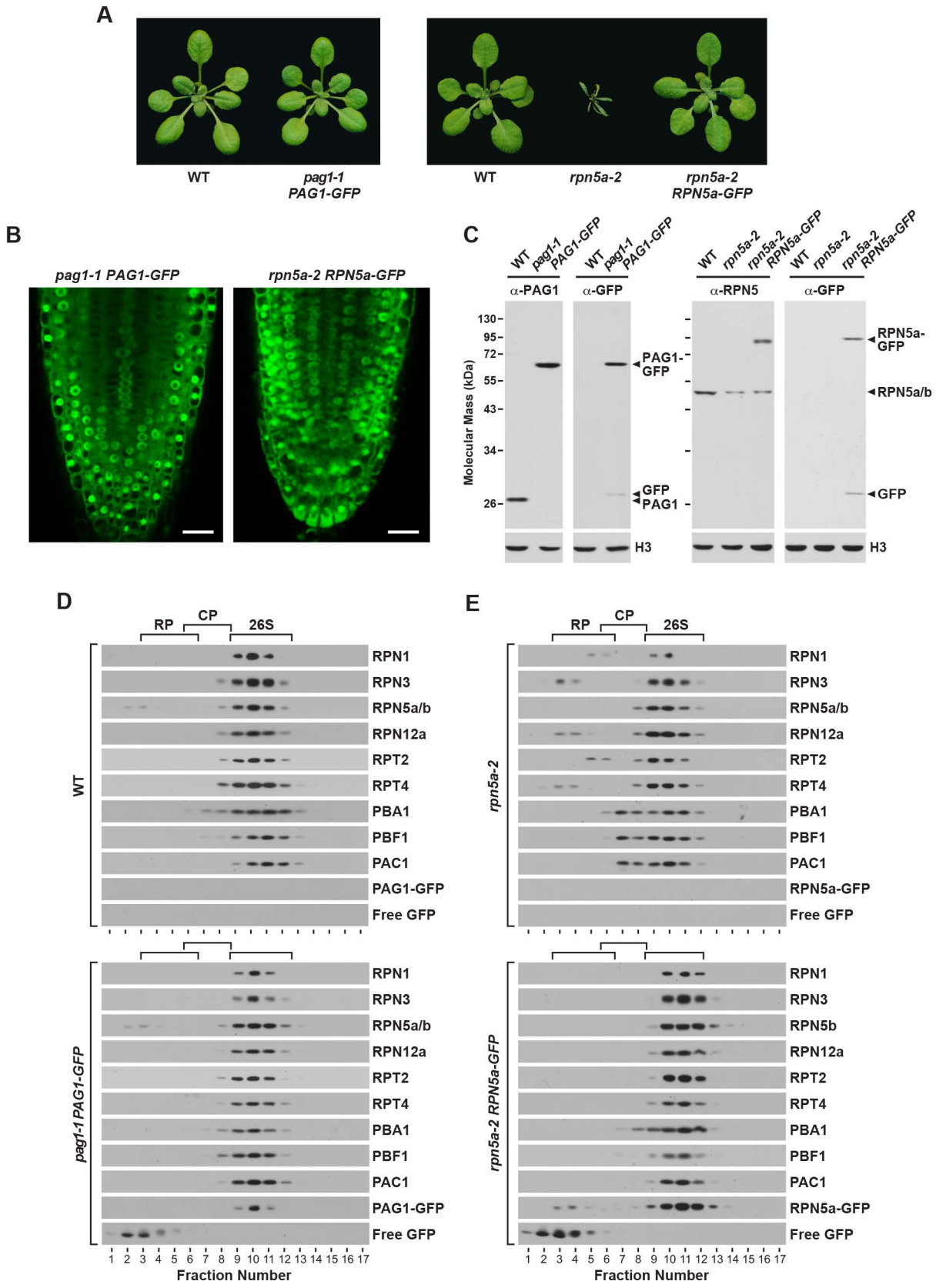

Figure S3. Marshall *et al.*

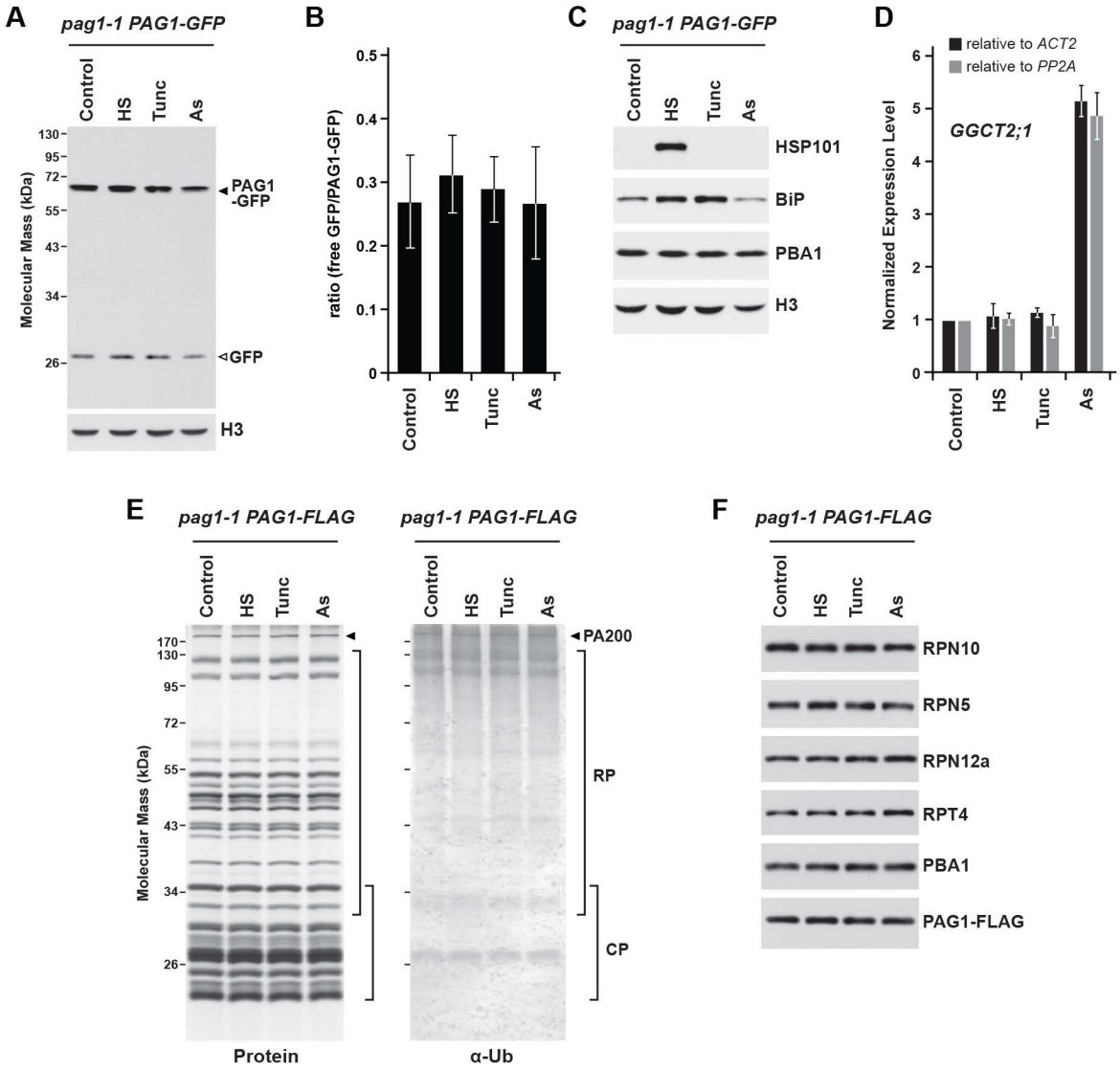

Figure S4. Marshall *et al.*

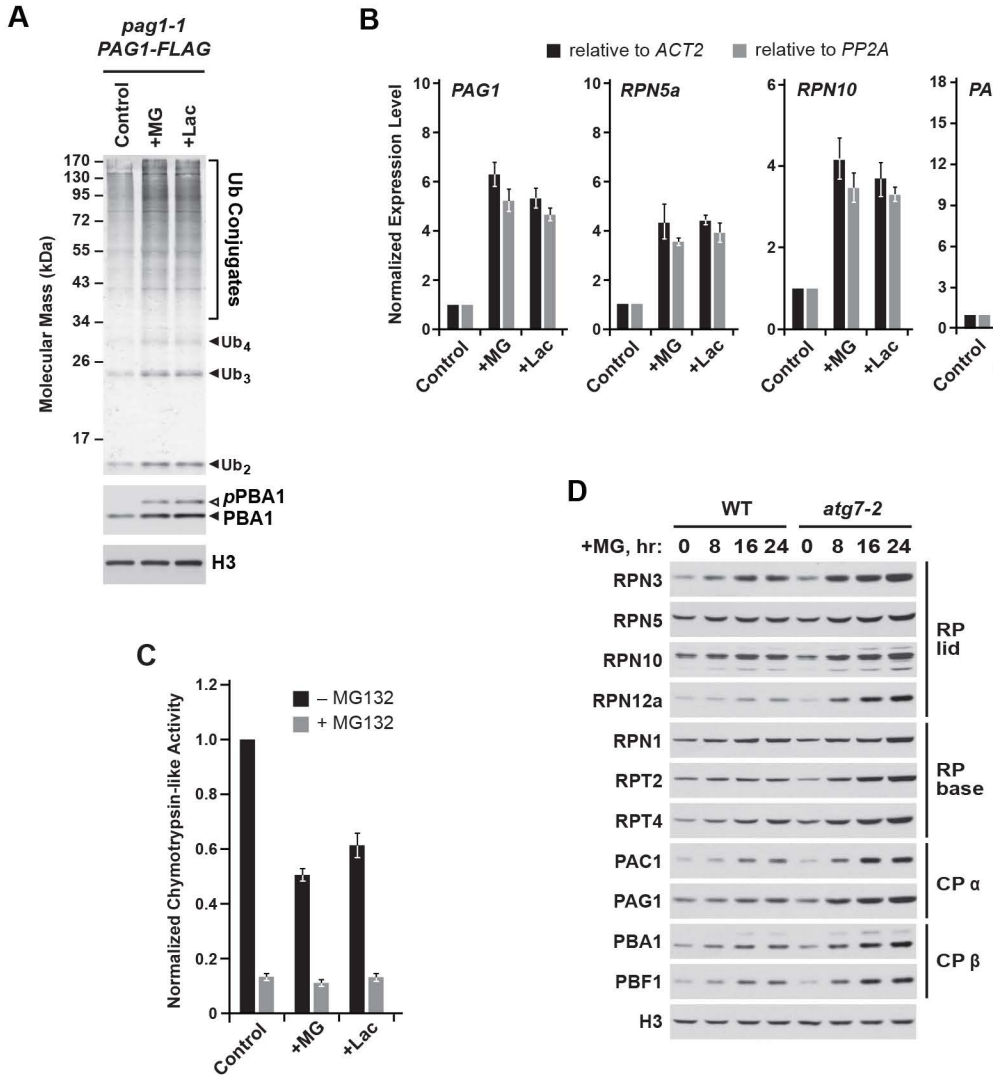

Figure S5. Marshall *et al.*

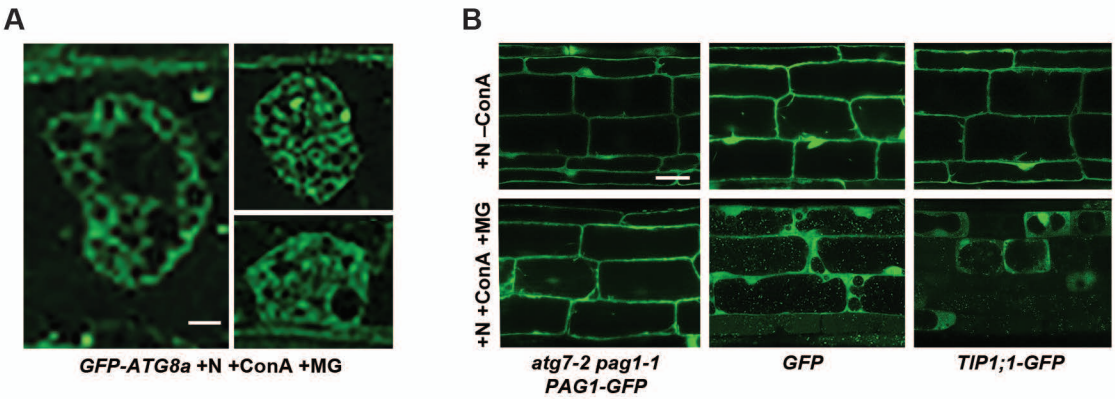

Figure S6. Marshall *et al.*

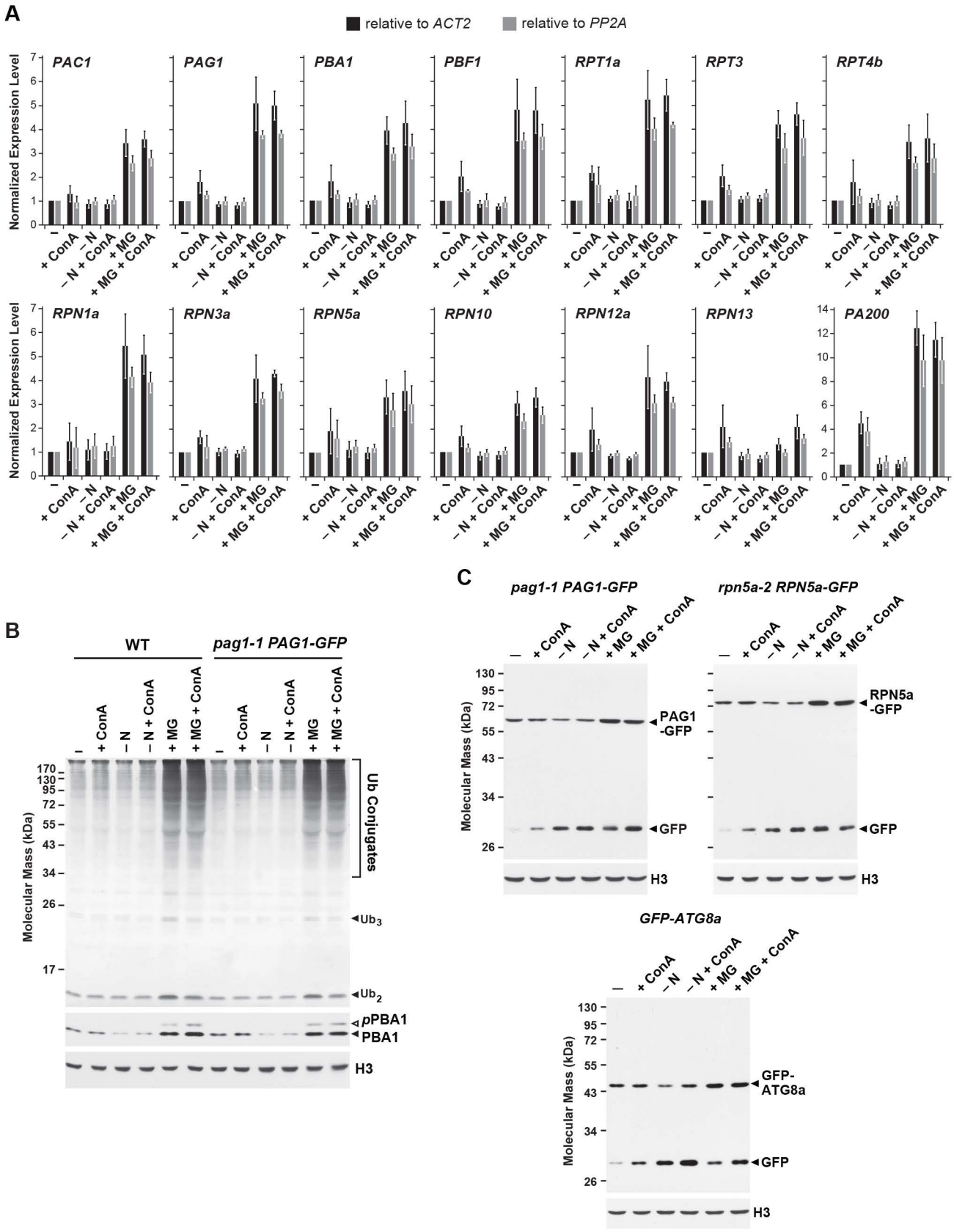

Figure S7. Marshall *et al.*

A

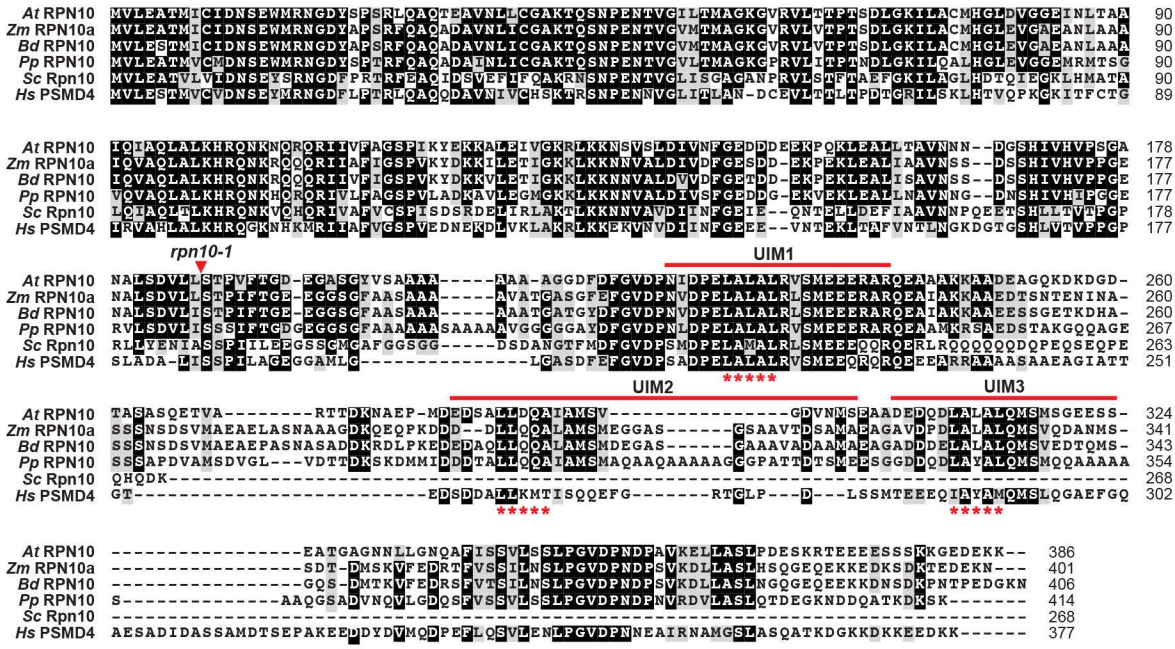

B

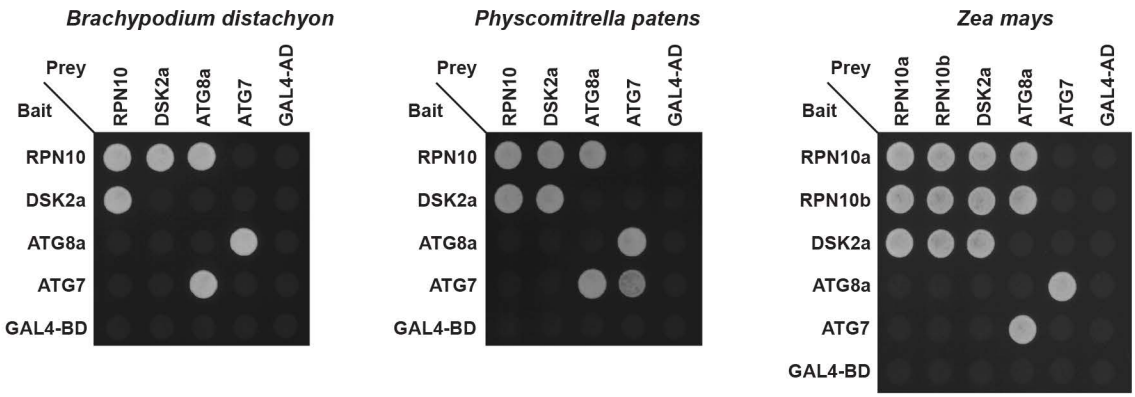

SUPPLEMENTAL FIGURE LEGENDS

Supplemental Figure 1. Proteasome gene expression, proteasome assembly and ubiquitin conjugate levels are unaltered in autophagy mutants. Related to Figure 1.

(A) Proteasome subunit genes are not transcriptionally up-regulated in autophagy mutants. Total RNA was extracted from 7-day-old WT or *atg* mutant seedlings and converted to first-strand cDNA. Relative transcript abundance of various proteasome subunit genes, including CP α- and β-subunits, RP base and lid subunits, and the alternate capping subunit PA200, was determined by quantitative real-time PCR, with the *ACT2* and *PP2A* genes used as reference standards. All data points were normalized to wild type (WT). Bars represent mean (±SD) from three biological replicates, each with three technical replicates.

(B) Proteasome assembly is not impaired in an autophagy mutant. Total protein extracts from 10-day-old WT or *atg7-2* seedlings were subjected to glycerol gradient centrifugation, fractionated, and samples of each fraction analyzed by SDS-PAGE followed by immunoblot with antibodies against various proteasome subunits. The expected positions of free CP, free RP, and the intact 26S proteasome are indicated by brackets. The assembly profile of proteasomes is largely the same in both WT and *atg7-2* seedlings.

(C) Native-PAGE analysis of 26S proteasomes affinity purified from autophagy mutants. Proteasomes were purified as in Figure 4A and then separated by native-PAGE in the presence of both ATP and $MgCl_2$. The gel was then stained for total protein with silver. The positions of the free CP, the CP capped with PA200, the free RP, and singly or doubly capped 26S proteasomes (26S-RP1 and 26S-RP2, respectively) are indicated. No differences in proteasome composition were observed in the autophagy mutants.

(D) Ubiquitin conjugate levels are unchanged in the autophagy mutants. Immunoblot detection of ubiquitin conjugates in total protein extracts from 10-day-old WT or homozygous autophagy mutant seedlings. Detection of histone H3 was used to confirm equal protein loading. The position of the higher molecular weight ubiquitin conjugates is indicated by the bracket.

Supplemental Figure 2. PAG1-GFP and RPN5a-GFP rescue the respective null phenotypes and are incorporated into 26S proteasomes. Related to Figure 1.

(A) Expression of *PAG1-GFP* and *RPN5a-GFP* from their native promoters rescues their respective T-DNA null phenotypes. *Arabidopsis* plants of the indicated genotypes were grown for 4 weeks under a long-day photoperiod prior to imaging. *PAG1-GFP* rescues the embryo lethality of the *pag1-1* T-DNA insertion, while *RPN5a-GFP* rescues the severe dwarf phenotype of *rpn5a-2*.

(B) The PAG1-GFP and RPN5a-GFP proteins are localized to the cytosol and nucleus in *Arabidopsis* root tip cells. Shown are confocal fluorescence microscopy images from 7-day-old seedlings of the indicated genotype grown in liquid medium under constant light. Scale bars represent 25 μm.

(C) Immunoblot analysis confirms expression of the *PAG1-GFP* and *RPN5a-GFP* transgenes. Total protein extracts from seedlings of the indicated genotypes were analyzed by SDS-PAGE, followed by immunoblot with antibodies against PAG1, RPN5, or GFP. In plants expressing *PAG1-GFP*, the endogenous PAG1 protein is absent, but is replaced by a higher molecular mass species corresponding to PAG1-GFP. In plants expressing *RPN5a-GFP*, levels of the endogenous protein are reduced (but not absent, due to the remaining RPN5b isoform), and a higher molecular mass species corresponding to RPN5a-GFP is observed. Detection of histone H3 was used to confirm near equal protein loading.
(D) PAG1-GFP and RPN5a-GFP are efficiently incorporated into 26S proteasomes. Total protein extracts from 10-day-old seedlings of the indicated genotypes were subjected to glycerol gradient centrifugation, fractionated, and samples of each fraction analyzed by SDS-PAGE followed by immunoblot with antibodies against various proteasome subunits and GFP. The expected positions of free CP, free RP, and the intact 26S proteasome are indicated by brackets. PAG1-GFP and RPN5a-GFP are observed in the same fractions as all other proteasome subunits, indicating that they assemble into the 26S complex. In wild-type plants and plants expressing *PAG1-GFP* and *RPN5a-GFP*, all subunits are found in fractions corresponding to the 26S proteasome, unlike in *rpn5a-2* plants, where many subunits are observed further up the gradient in regions corresponding to free CP or RP, indicative of impaired proteasome assembly. In both lines, free GFP was detected towards the top of the gradient.

Supplemental Figure 3. Proteotoxic stress does not affect proteasome ubiquitylation or proteaphagic turnover. Related to Figure 3.
(A) Proteophagy rates are unchanged in response to treatments that induce proteotoxic stress. 7-day-old seedlings expressing *PAG1-GFP* were subjected to heat shock (HS), tunicamycin (Tunc) or arsenite (As) treatment, and then analyzed by SDS-PAGE and immunoblot with anti-GFP antibodies. The positions of PAG1-GFP and free GFP are indicated by black and white arrowheads, respectively. None of the treatments caused any change in the levels of free GFP. Detection of histone H3 was used to confirm near equal protein loading.
(B) Quantification of the ratio of free GFP to PAG1-GFP from the experiment shown in A, plus two additional biological replicates. Bars represent the mean (±SD) of the three biological replicates.
(C) Control immunoblots confirmed the effectiveness of the heat shock and tunicamycin treatments. Seven-day-old seedlings treated as in A were analyzed by SDS-PAGE followed by immunoblot with the indicated antibodies. HSP101 accumulates dramatically in response to heat shock, whereas BiP levels increase in response to both heat shock and tunicamycin treatment. Proteasome activity appeared unimpaired, as no unprocessed PBA1 was seen to accumulate. Detection of histone H3 was used to confirm near equal protein loading.
(D) Transcript levels of the γ-glutamyl cyclotransferase gene *GGCT2;1* confirm the effectiveness of sodium arsenite treatment. Total RNA was extracted from 7-day-old seedlings treated as in A, and then converted to cDNA. Relative transcript abundance was determined by quantitative real-time

PCR, with the *ACT2* and *PP2A* genes used as reference standards. All data points were normalized to the untreated *PAG1-GFP* seedlings (control). Bars represent mean (±SD) from three biological replicates, each with three technical replicates.

(E) Proteasome ubiquitylation does not change in response to treatments that induce proteotoxic stress. 26S proteasomes were affinity purified from 10-day-old seedlings expressing *PAG1-FLAG* treated as in A, and then analyzed by SDS-PAGE followed by silver staining or immunoblot with anti-ubiquitin antibodies. The alternate capping particle PA200 is indicated by an arrowhead, and the positions of other CP and RP subunits are indicated by brackets. No increase in proteasome ubiquitylation was observed in the treated samples.

(F) Proteotoxic stress does not lead to an increased proteasomal association of RPN10. 26S proteasomes affinity purified as in E were analyzed by SDS-PAGE and immunoblot with antibodies against various proteasome subunits. The anti-FLAG blot demonstrated equal efficiency of pulldown between the different samples, and levels of all other subunits analysed were unchanged by the different treatments.

Supplemental Figure 4. MG132 and *clasto*-lactacystin β-lactone increase levels of ubiquitin conjugates and activate the proteasome-stress regulon. Related to Figure 3.

(A) Ubiquitin conjugate levels are increased following proteasome inhibition. Total protein extracts from 10-day-old seedlings treated with or without 50 μM MG132 or *clasto*-lactacystin β-lactone for 16 hours were subjected to SDS-PAGE followed by immunoblot analysis with anti-ubiquitin or anti-PBA1 antibodies. The positions of ubiquitin chains and ubiquitin conjugates are indicated by arrowheads and a bracket, respectively. Treatment with both inhibitors caused the accumulation of ubiquitin conjugates and the appearance of unprocessed PBA1. Detection of histone H3 was used to confirm near equal protein loading.

(B) Transcript levels of various proteasome subunit genes are increased in response to proteasome inhibition. Total RNA was extracted from 7-day-old seedlings treated as in A, and then converted to cDNA. Relative transcript abundance of the indicated proteasome subunit genes was determined by quantitative real-time PCR, with the *ACT2* and *PP2A* genes used as reference standards. All data points were normalized to the untreated *PAG1-FLAG* seedlings (control). Bars represent mean (±SD) from three biological replicates, each with three technical replicates.

(C) Levels of active 26S proteasomes are reduced upon inhibitor treatment. Total protein extracts from 7-day-old seedlings treated as in A were assayed for chymotrypsin-like peptidase activity in the presence or absence of 80 μM MG132, using the fluorogenic substrate succinyl-Leu-Leu-Val-Tyr-7-amido-4-methylcoumarin. Activity was normalized to untreated wild type (control) in the absence of MG132. Bars represent mean (±SD) from three biological replicates, each with three technical replicates.

(D) MG132 treatment induces an increase in the levels of 26S proteasome components, which is enhanced in an autophagy mutant. Wild type (WT) and *atg7-2* seedlings were grown for 6 days and then treated with MG132 for the indicated times. Total protein extracts were probed with antibodies against various CP and RP subunits. Detection of histone H3 was used to confirm near equal protein loading.

Supplemental Figure 5. Formation of the distorted vacuolar structures seen upon MG132 and ConA treatment is dependent on autophagy. Related to Figure 3.

(A) High magnification images of the distorted vacuolar structures seen upon MG132 and ConA treatment (see Figure 3C). Seven-day-old seedlings expressing *GFP-ATG8a* were treated with 50 μM MG132 and 1 μM ConA for 16 hours and imaged by confocal fluorescence microscopy. Scale bar = 2 μm.

(B) Formation of the structures seen in root cells upon MG132 and ConA treatment is dependent on autophagy, but they are not derived from cytosol or tonoplast. Seedlings of the indicated genotypes were treated with 50 μM MG132 and 1 μM ConA as in A, and imaged by confocal fluorescence microscopy. The distorted structures were not observed in plants expressing free GFP or the tonoplast marker TIP1;1-GFP, nor in plants expressing PAG1-GFP in the *atg7-2* mutant back-ground. Scale bar = 10 μm.

Supplemental Figure 6. Proteasome inhibition and nitrogen starvation both stimulate proteaphagy. Related to Figure 3.

(A) Proteasome subunit gene transcription is up-regulated upon MG132 treatment, but not upon nitrogen starvation or treatment with ConA. Total RNA was extracted from wild-type (WT) seedlings grown for 6 days and then treated with or without combinations of nitrogen starvation, 1 μM ConA and/or 50 μM MG132 for 16 hours. RNA was then converted to first-strand cDNA, and the relative transcript abundance of various proteasome subunit genes, including CP α- and β-sub-units, RP base and lid subunits, and the alternate capping subunit PA200, was determined by quantitative real-time PCR, with *ACT2* and *PP2A* genes used as reference standards. All data points were normalized to untreated WT (control). Bars represent mean (±SD) from three biological replicates, each with three technical replicates.

(B) Total protein extracts from 10-day-old seedlings of the indicated genotype treated as in A were subjected to SDS-PAGE and immunoblot analysis with anti-ubiquitin or anti-PBA1 antibodies. The positions of ubiquitin chains and ubiquitin conjugates are indicated by arrowheads and a bracket, respectively. Treatment with MG132, but not with N starvation or ConA, caused accumulation of ubiquitin conjugates and the unprocessed form of PBA1. Detection of histone H3 was used to confirm near equal protein loading.

(C) Immunoblot detection of free GFP released during vacuolar breakdown of PAG1-GFP (see top left panel), RPN5a-GFP (top right panel), and GFP-ATG8a (lower panel). Seedlings of the indicated genotypes were grown for 6 days and then treated as in A. Total protein extracts were subjected to immunoblot analysis with anti-GFP antibodies. Closed and open arrowheads indicate fused-GFP and free GFP, respectively. Detection of histone H3 was used to confirm near equal protein loading.

Supplemental Figure 7. The RPN10-ATG8 interaction is conserved throughout the plant kingdom. Related to Figure 6.

(A) A sequence alignment of RPN10 proteins from *Arabidopsis thaliana*, *Brachypodium distachyon*, *Zea mays*, *Physcomitrella patens*, *Saccharomyces cerevisiae* and humans (where it is instead known as PSMD4). Identical amino acids (with a 60 % threshold value) are shown with a black background, while similar amino acids are shown with a grey background. The position of the previously described exon-trap mutant (*rpn10-1*) is indicated by the red arrowhead. The positions of the three ubiquitin-interacting motifs (UIM1-3) are indicated by red lines, whereas the amino acids mutated to abolish UIM binding activity are indicated by red asterisks.

(B) Y2H interactions between RPN10 and ATG8 from the three different plant species shown in A. The indicated full-length proteins fused with either the GAL4 activating (AD) or GAL4 binding (BD) domain at their N-terminus were co-expressed in the yeast strain MaV203 in all pairwise orientations, including with the GAL4 domains alone as controls. The known interactions between RPN10 and DSK2, and ATG8 and ATG7, were used as positive controls. Maize contains two isoforms of RPN10, of which both were tested in this assay. Details of other isoforms not examined here are given in Supplemental Table 4. The images show cells selected for growth on medium lacking tryptophan, leucine and histidine, and containing 25 mM 3-amino-1,2,4-triazole.

TABLE S1: T-DNA insertion lines used in this study. Related to Experimental Procedures.

Gene name	Locus[a]	Line name	Line ID[b]	Insertion site	Ecotype[c]	Reference[d]
ATG4a	At2g44140	*atg4a-2*	SAIL_740_H03	5th exon	Col-0	1
ATG4b	At3g59950	*atg4b-2*	SALK_056994	8th intron	Col-0	1
ATG5	At5g17290	*atg5-1*	SAIL_129_B07	4th intron	Col-3	2
ATG7	At5g45900	*atg7-2*	GABI_655_B06	7th exon	Col-0	3
ATG10	At3g07525	*atg10-1*	SALK_084434	4th exon	Col-0	4
ATG11	At4g30790	*atg11-1*	SAIL_1166_G10	2nd exon	Col-3	5
ATG12a	At1g54210	*atg12a-1*	SAIL_1287_A08	3rd exon	Col-0	1
ATG12b	At3g13970	*atg12b-1*	SALK_003192	4th intron	Col-0	1
ATG13a	At3g49590	*atg13a-2*	SALK_044831	1st exon	Col-0	6
ATG13b	At3g18770	*atg13b-2*	GABI_501_F06	2nd intron	Col-0	6
NBR1	At4g24690	*nbr1-2*	GABI_246_H08	3rd exon	Col-0	7
PAG1	At2g27020	*pag1-1*	SALK_114864	5th intron	Col-0	8
RPT2a	At4g29040	*rpt2a-2*	SALK_005596	4th exon	Col-0	9
RPT4b	At1g45000	*rpt4b-2*	SALK_101982	2nd exon	Col-0	This study
RPN5a	At5g09900	*rpn5a-2*	SALK_010840	3rd exon	Col-0	10
RPN10	At4g38630	*rpn10-1*	SL41-45	5th intron	C24	11

[a] Locus identifiers are taken from the Arabidopsis Information Resource (www.arabidopsis.org).

[b] T-DNA collections are described in: Sessions *et al.*, 2002 (SAIL); Alonso *et al.*, 2003 (SALK); Kleinboelting *et al.*, 2012 (GABI-Kat); Babiychuk *et al.*, 1997 (exon trap mutants).

[c] Lines were backcrossed 3 times to Col-0 before analysis.

[d] References are: 1. Chung *et al.*, 2010; 2. Thompson *et al.*, 2005; 3. Hofius *et al.*, 2009; 4. Phillips *et al.*, 2008; 5. Li *et al.*, 2014; 6. Suttangkakul *et al.*, 2011; 7. Zhou *et al.*, 2013; 8. Book *et al.*, 2010; 9. Ueda *et al.*, 2004; 10. Book *et al.*, 2009; 11. Smalle *et al.*, 2003.

TABLE S2: Transgenic *Arabidopsis* lines used in this study. Related to Experimental Procedures.

Genotype[a]	Construct type	Transformation vector[b]	Antibiotic resistance	Reference[c]
pag1-1 PAG1::PAG1-FLAG	Genomic	pEarleyGate302	BASTA	1
pag1-1 PAG1::PAG1-GFP	Genomic	pMDC107	Hygromycin	This study
rpn5a-2 RPN5a::RPN5a-GFP	Genomic	pMDC107	Hygromycin	This study
35S::GFP	cDNA	pKGWFS7	Kanamycin	Provided by Shih-Heng Su
35S::GFP-ATG8a	cDNA	pEGAD	BASTA	2
UBQ10::mCherry-ATG8a	cDNA	pMDC99	Hygromycin	3
35S::TIP1;1-GFP	cDNA	pBIN20	Kanamycin	4

[a] All constructs were transformed into the Col-0 ecotype via the floral dip method (Clough and Bent, 1998).

[b] Plant transformation vectors are described in: Earley *et al.*, 2006 (pEarleyGate series); Curtis and Grossnik-laus (pMDC series); Karimi *et al.*, 2002 (pKGWFS7); Cutler *et al.*, 2000 (pEGAD); Hennegan and Donna, 1998 (pBIN20).

[c] References are: 1. Book *et al.*, 2010; 2. Thompson *et al.*, 2005; 3.Suttangkakul *et al.*, 2011; 4. Nelson *et al.*, 2007.

TABLE S3: Oligonucleotide primers used in this study. Related to Experimental Procedures.

See separate Excel spreadsheet.

TABLE S4: Accession numbers of genes used in this study. Related to Figure S7.

Name	Species	Accession Number[a]	Additional gene isoforms not examined in this study[b]
ATG4a	*Arabidopsis thaliana*	At2g44140	N/A
ATG4b	*Arabidopsis thaliana*	At3g59950	
ATG5	*Arabidopsis thaliana*	At3g51830	N/A
ATG7	*Arabidopsis thaliana*	At5g45900	N/A
ATG8a	*Arabidopsis thaliana*	At4g21980	ATG8b (At4g04620) ATG8c (At1g62040) ATG8d (At2g05630) ATG8g (At3g60640) ATG8h (At3g06420)
ATG8e	*Arabidopsis thaliana*	At2g45170	
ATG8f	*Arabidopsis thaliana*	At4g16520	
ATG8i	*Arabidopsis thaliana*	At3g15580	
ATG10	*Arabidopsis thaliana*	At3g07525	N/A
ATG11	*Arabidopsis thaliana*	At4g30790	N/A
ATG12a	*Arabidopsis thaliana*	At1g54210	N/A
ATG12b	*Arabidopsis thaliana*	At3g13970	
ATG13a	*Arabidopsis thaliana*	At3g49590	N/A
ATG13b	*Arabidopsis thaliana*	At3g18770	
NBR1	*Arabidopsis thaliana*	At4g24690	N/A
PAC1	*Arabidopsis thaliana*	At3g22110	PAC2 (At4g15160)
PAG1	*Arabidopsis thaliana*	At2g27020	N/A
PBA1	*Arabidopsis thaliana*	At4g31300	N/A
PBF1	*Arabidopsis thaliana*	At3g60820	N/A
RPT1a	*Arabidopsis thaliana*	At1g53750	RPT1b (At1g53780)
RPT3	*Arabidopsis thaliana*	At5g58290	N/A
RPT4b	*Arabidopsis thaliana*	At1g45000	RPT4a (At5g43010)
RPN1a	*Arabidopsis thaliana*	At2g20580	RPN1b (At4g28470)

RPN3a	*Arabidopsis thaliana*	At1g20200	RPN3b (At1g75990)
RPN5a	*Arabidopsis thaliana*	At5g09900	RPN5b (At5g64760)
RPN10	*Arabidopsis thaliana*	At4g38630	N/A
RPN12a	*Arabidopsis thaliana*	At1g64520	RPN12b (At5g42040)
RPN13	*Arabidopsis thaliana*	At2g26590	N/A
PA200	*Arabidopsis thaliana*	At3g13330	N/A
RPN10	*Brachypodium distachyon*	Bradi1g68290	N/A
DSK2	*Brachypodium distachyon*	Bradi1g76314	Bradi1g76321
ATG8	*Brachypodium distachyon*	Bradi3g14980	Bradi0098s00200 Bradi1g26400 Bradi4g45390
ATG7	*Brachypodium distachyon*	Bradi2g43480	N/A
RPN10a	*Zea mays*	GRMZM2G147671	N/A
RPN10b	*Zea mays*	GRMZM2G165926	
DSK2	*Zea mays*	GRMZM2G136769	GRMZM2G127101 GRMZM2G170843
ATG8a	*Zea mays*	GRMZM2G336871	ATG8b (GRMZM2G076826) ATG8c (GRMZM2G419694) ATG8d (GRMZM2G134613) ATG8e (GRMZM2G014975)
ATG7	*Zea mays*	GRMZM2G005304	N/A
RPN10	*Physcomitrella patens*	Phpat.006G076300	N/A
DSK2	*Physcomitrella patens*	Phpat.004G024000	Phpat.008G018100 Phpat.012G049300
ATG8	*Physcomitrella patens*	Phpat.014G056800	Phpat.001G128200 Phpat.014G057000 Phpat.014G057100 Phpat.017G019100
ATG7	*Physcomitrella patens*	Phpat.024G027800	N/A

[a] Accession numbers are taken from the *Arabidopsis* Information Resource (www.arabidopsis.org) or Phytozome (www.phytozome.net). [b] N/A; not applicable.

SUPPLEMENTAL EXPERIMENTAL PROCEDURES

Plant materials and growth conditions

Unless otherwise noted, all *Arabidopsis thaliana* seeds (ecotype Col-0) were vapour-phase sterilized, vernalized at 4 °C for 3-4 days, and germinated on solid GM medium (3.2 g/l Gamborg's B5 basal salts, 1 % (w/v) sucrose, 0.05 % (w/v), MES (pH 5.7), 0.7 % (w/v) agar) at 21-23 °C under a long-day photoperiod (16-hours light/8-hours dark, with a light intensity of 75-100 µmol/m^2/sec). For selection of transgenic plants, agar plates were supplemented with appropriate combinations of antibiotics or herbicide (50 µg/ml kanamycin, 25 µg/ml hygromycin, 6 µg/ml sulphadiazine or 10 µg/ml BASTA). After 2-3 weeks, seedlings were transferred to soil (mixed in a 1:1 ratio with organic Coco Coir planting mixture, supplemented before use with 2 g/l Peters 20-20-20 fertilizer, 80 mg/l $Ca(NO_3)_2$, and 80 mg/l $MgSO_4$) and grown at 21-23 °C under a long-day photoperiod.

For chemical treatment, seedlings were grown in liquid GM medium (as above, but without agar) at 21-23 °C under continuous light with gentle shaking (90 rpm), with medium replenished every 3 days where required. On the sixth or ninth day, fresh medium was supplemented with the indicated concentrations of concanamycin A (Santa Cruz Biotechnology, 0.5 mM stock in DMSO), MG132 (Selleckchem, 50 mM stock in DMSO), *clasto*-lactacystin β-lactone (Sigma-Aldrich, 50 mM stock in DMSO), sodium arsenite (Sigma-Aldrich, 50 mM stock in H_2O), or tunicamycin (Sigma-Aldrich, 5 mg/ml stock in DMSO), with equivalent volumes of DMSO or water as controls. For nitrogen starvation experiments, seedlings were grown in liquid MS medium (4.4 g/l Murashige and Skoog basal medium, 1 % (w/v) sucrose, 0.05 % (w/v) MES (pH 5.7)), before transfer to fresh MS medium or MS medium lacking nitrogen (MS basal salt micronutrient solution (Sigma-Aldrich) supplemented with 3 mM $CaCl_2$, 1.5 mM $MgSO_4$, 1.25 mM KH_2PO_4, 5 mM KCl, 1 % (w/v) sucrose, 0.05 % (w/v) MES (pH 5.7)) for the indicated times. Both control and treated seedlings were washed three times in fresh medium prior to treatment. Heat shock treatment was performed by incubating 7- or 10-day-old liquid cultures at 37 °C for 30 minutes with gentle shaking, followed by a 30 minute recovery at 21-23 °C. Following treatment, tissue was harvested, immediately frozen to liquid nitrogen temperatures, and stored at -80 °C before analysis.

All T-DNA insertion mutants were confirmed by genomic PCR using 5′ and 3′ gene-specific primers (LP and RP, respectively) in conjunction with an appropriate T-DNA left border-specific primer (BP). Details of all primers used in this study are provided in Supplemental Table 3. Before analysis, each mutant was backcrossed three times to wild-type Col-0 and then selfed to obtain homozygous progeny. Transgenes expressing *PAG1-GFP* and *RPN5a-GFP* under the control of their native promoters were generated by PCR amplification of the respective genomic sequences (from 2 kb upstream of the ATG translation start site to the final codon prior to the TAA or TAG stop codon, respectively) from Col-0 DNA. The PCR products were recombined into the pENTR™/D-TOPO® vector (Life Technologies), and sequence-confirmed clones were recombined in-frame with GFP at

their 3′ end in the pMDC107 vector (Curtis and Grossniklaus, 2003) via the Gateway® LR clonase™ II reaction (Invitrogen). The constructs were then introduced into *Agrobacterium tumefaciens* strain GV3101, and heterozygous *pag1-1* or *rpn5a-2* plants were transformed by *Agrobacterium*-mediated floral dip (Clough and Bent, 1998). Hygromycin-resistant F_1 plants were confirmed by PCR genotyping to contain the *pag1-1* or *rpn5a-2* allele. After a self cross, double homozygous plants containing both the mutation and the transgene were identified in the F_2 generation by PCR genotyping, segregation of the F_3 generation on hygromycin-containing medium, and by confocal laser scanning microscopy (see below). Details of all other previously published stable transgenic lines used in this study are given in Supplemental Table 2. Plants expressing transgenes in the various *atg*, *rpt* or *rpn* mutant backgrounds were generated by introgression.

Tobacco (*Nicotiana benthamiana*) plants for *Agrobacterium*-mediated leaf infiltration were sown directly onto soil (as above), vernalized at 4 °C for 3-4 days, and grown at 21-23 °C under a 12-hour light/12-hour dark cycle. Plants were re-fertilized once a week.

Immunological techniques

Frozen tissue samples were homogenized in 3 volumes of protein extraction buffer (50 mM Tris-HCl (pH 7.5), 150 mM NaCl, 2 mM dithiothreitol, 1 mM phenylmethylsulphonyl fluoride, 50 μM MG132, 1 × protease inhibitor cocktail (Sigma-Aldrich)) and clarified by centrifugation at 13,000 × *g* for 5 minutes at 4 °C. The supernatant was mixed with 5 × SDS-PAGE sample buffer (200 mM Tris-HCl (pH 6.8), 25 % (v/v) glycerol, 10 % (w/v) SDS, 10 % (v/v) β-mercaptoethanol, 0.005 % (w/v) bromophenol blue), and the samples were heated at 95 °C for 5 minutes prior to gel analysis.

Following SDS-PAGE, gels were either stained for protein with silver or subjected to immunoblot analysis following transfer to polyvinylidene difluoride membranes (Millipore). Antibodies against RPN1 (Yang *et al.*, 2004), RPN5, RPN12, RPT2, PAC1, PBA1, PBF1 (Smalle *et al.*, 2002), RPN10, ubiquitin (Van Nocker *et al.*, 1996a), PAG1, PA200 (Book *et al.*, 2010), CDC48 (Rancour *et al.*, 2002), HSP101 (Hong and Vierling, 2001), and tobacco BiP (Pedrazzini *et al.*, 1997) were previously described, while antibodies against RPN3 and RPT4 were provided by Kwang-Hee Lee (University of Wisconsin). Antibodies against FLAG, GST and histone H3 were purchased from Sigma-Aldrich (product number F1804), Santa Cruz Biotechnology (product number SC138) and AbCam (product number AB1791), respectively, while a combination of monoclonal antibodies against GFP was purchased from Roche Diagnostics (product number 11814460001). Goat anti-rabbit or anti-mouse secondary antibodies conjugated to horseradish peroxidise or alkaline phosphatase were obtained from KPL, with the rabbit anti-chicken IgY-HRP conjugate provided by Sebastian Y. Bednarek (University of Wisconsin).

Blots were developed using SuperSignal® West Pico Chemiluminescent Substrate or SuperSignal® West Femto Maximum Sensitivity Substrate (Thermo Scientific), as according to the manufacturers instructions, or by combining 100 mg/ml nitro-blue tetrazolium and 50 mg/ml 5-bromo-4-

chloro-3-indolylphosphate (both from Research Products International) in alkaline phosphatase development buffer (100 mM diethanolamine, 100 mM NaCl, 5 mM $MgCl_2$, pH 9.5), applying this uniformly to the membrane, and incubating at room temperature for 10-30 minutes. Densitometric quantification of blots was performed using TotalLab™ software (Non-linear Dynamics), with at least three different exposures of the same blot being quantified to ensure the exposure level was within the linear range of the film.

Quantitative real-time PCR analysis

Total RNA was extracted from 50-100 mg of 10-day-old plate grown or 7-day-old liquid grown seedlings using the RNeasy® plant mini kit (QIAGEN), as according to the manufacturer's instructions. Following quantification with a NanoDrop™ 1000 spectrophotometer (Thermo Scientific), 1 µg of total RNA was treated with DNase I (Invitrogen), and RNA integrity was assessed by a combination of OD_{260}/OD_{280} and OD_{260}/OD_{230} measurements, and by running samples on a denaturing formaldehyde agarose gel. RNA was converted to cDNA using the SuperScript® III first-strand synthesis system (Invitrogen) and oligo$(dT)_{20}$ primers, again as according to the manufacturer's instructions. Quantitative real-time PCR of 26S proteasome subunit transcripts was performed on three independent biological replicates using a LightCycler® 480 machine (Roche Diagnostics) and LightCycler® 480 SYBR Green I master mix (Roche Diagnostics), with three technical replicates for each reaction. In all cases, the amplification factor of the primer pair was experimentally determined to be between 1.90 and 2.10, with the gradient of the standard curve being between -3.59 and -3.10, and the R^2 value being greater than 0.950. For each individual PCR reaction, 5 µl of cDNA (diluted 1/30 following first-strand synthesis) was amplified in a 20 µl reaction volume also containing 10 µl SYBR Green I master mix, 3 µl sterile H_2O, and 1 µl each of 10 µM forward and reverse primers. Reaction parameters were 95 °C for 5 minutes, 45 cycles of 95 °C for 10 seconds, 55 °C for 10 seconds and 72 °C for 30 seconds, followed by a melting curve program and cooling at 40 °C for 2 minutes. Fluorescence data were collected at the end of each 72 °C extension step, and continuously during the melting curve program (Bustin et al., 2009). The relative transcript abundance of target genes was determined using the comparative threshold cycle method (Pfaffl, 2001) using the *ACT2* and *PP2A* reference genes as internal controls (Czechowski et al., 2005; Remans et al., 2014), and all data was normalized to untreated Col-0.

Glycerol gradient centrifugation and proteasome activity assays

Glycerol gradient fractionations were performed essentially as previously described (Book *et al.*, 2009), with minor modifications. Seedlings were grown in 5 ml of liquid GM medium at 21-23 °C under continuous light for 10 days with gentle shaking (90 rpm). Typically, ~30 mg of dry seeds were used per culture, resulting in ~2 g of fresh weight tissue. Frozen seedling tissue was ground to a fine powder and proteins were extracted with 1 volume of Buffer A (20 mM Tris-HCl (pH 7.5), 5 mM

$MgCl_2$, 10 % (v/v) glycerol, with 2 mM ATP, 1 mM dithiotreithol, 10 mM phosphocreatine and 1 mg/ml creatine phosphokinase (Sigma-Aldrich) added immediately before use). Extracts were filtered through two layers of Miracloth (Calbiochem) and clarified at 30,000 × *g* for 20 minutes at 4 °C. 1 ml of supernatant was loaded onto an 11 ml, 10 % to 40 % (v/v) glycerol density gradient in Buffer A, made with an Auto Densi-Flow density gradient fractionator (Labconco). Following centrifugation at 100,000 × *g* for 18 hours at 4 °C, 500 µl fractions were manually collected with a Gilson-type P1000 pipette, and 10 µl of each fraction was subjected to SDS-PAGE and immunoblot analysis.

To assay 26S proteasome activity, proteasomes were first partially purified from *Arabidopsis* seedlings. Following the clarification step described above, the supernatant was made 10 % (w/v) in PEG 8000 (from an initial stock of 40 %) and incubated for 30 minutes at 4 °C. The precipitate was collected by centrifugation at 12,000 × *g* for 15 minutes at 4 °C and resuspended in 500 µl of buffer A, a step which has been shown to remove the majority of lower molecular weight proteases that may interfere with the assay (Yang *et al.*, 2004). The total protein concentration of each sample was determined by Pierce™ BCA protein assay kit (Thermo Scientific), and equal amounts of protein (10 µg) from each sample were assayed for proteasome activity in the presence or absence of 80 µM MG132 (Kisselev and Goldberg, 2005). Protein samples in a volume of 20 µl were incubated for 20 minutes at 37 °C in 1 ml of assay buffer (50 mM Tris-HCl (pH 7.0), 2 mM $MgCl_2$, with 1 mM ATP and 2 mM β-mercaptoethanol added immediately before use) containing 100 µM of the fluorogenic substrate N-succinyl-leucyl-leucyl-valyl-tyrosyl-7-amino-4-methylcoumarin (succinyl-LLVY-AMC, Sigma-Aldrich). Reactions were quenched by the addition of 1 ml 80 mM sodium acetate (pH 4.3), and the fluorescence of released AMC was monitored using a TKO 100 fluorometer (Hoefer Scientific Instruments), with an excitation wavelength of 365 nm and an emission wavelength of 460 nm. Three technical replicates were assayed for each sample, and the data from three biological replicates were averaged and normalized to the activity observed in Col-0 tissue in the absence of MG132.

Confocal laser scanning microscopy and image analysis

Seedlings of the indicated genotype were grown in 5 ml liquid GM media at 21-23 °C under continuous light for 6 days with gentle shaking (90 rpm) before being transferred to fresh medium either containing or lacking nitrogen, and supplemented with the indicated combinations of 1 µM ConA, 50 µM MG132, 20 µM MVB003, 20 µM MVB072, or 20 µM epoxomycin (or equivalent volumes of DMSO as a control). Following incubation for the indicated periods of time, root cells within the lower elongation zone were visualized with a Zeiss 510 Meta confocal laser scanning microscope, using 488 nm light combined with the 500-530 nm infra-red band-pass filters for the GFP images, 488 nm light combined with the 500-550 nm infra-red band-pass filters for YFP images, and 543 nm light combined with the 565-615 nm infra-red band-pass filters for the mCherry, MVB003 and MVB072 images. All images were scanned in single track mode, except for co-localisation studies, when the GFP and mCherry signals were instead detected simultaneously in multi-track mode. Microscopy images

were processed using the Zeiss LSM 510 Image Browser and/or Adobe Photoshop CC, and were converted to TIFF files for use in figures. Within each figure, all images were captured using identical microscope settings, with the exception of bright field images, where the channel gain was adjusted to provide uniform exposure between images.

Protein-protein interactions were assessed *in planta* using bimolecular fluorescence complementation (Citovsky *et al.*, 2006; Ohad *et al.*, 2007). Full-length cDNAs of the indicated *Arabidopsis* genes were amplified by PCR and then recombined into pDONR™221 (Life Technologies) via the Gateway® BP clonase™ II reaction (Invitrogen). These cDNAs were recombined in-frame to the N- or C-terminal halves of EYFP in the pSITE-N-EYFP-C1 or pSITE-C-EYFP-C1 vectors (ABRC stock numbers CD3-1648 and CD3-1649, respectively (Martin *et al.*, 2009)) via the Gateway® LR clonase™ II reaction (Invitrogen), with expression driven by the cauliflower mosaic virus *35S* promoter. The constructions were verified by sequencing and introduced into *Agrobacterium tumefaciens* strain GV3101, cultures of which were then used for direct infiltration of *Nicotiana benthamiana* leaves, as previously described (Sparkes *et al.*, 2006). Where indicated, a second infiltration of buffer containing ConA was performed ~24 hours later. Leaf sections were excised ~36 hours after the initial infiltration and visualized as described above.

Proteasome affinity purifications

Affinity purification of 26S proteasomes from *Arabidopsis* seedlings was performed essentially as previously described (Book *et al.*, 2010), with minor modifications. Seedlings of the indicated genotype were liquid-phase sterilized following a 30-minute imbibition in sterile water, vernalized at 4 °C for 4-5 days, and grown in 50 ml of liquid GM medium at 21-23 °C under continuous light for 10 days with gentle shaking (90 rpm). Where indicated, the medium was removed on the ninth day and replenished with fresh medium containing 50 μM MG132, 50 μM *clasto*-lactacystin β-lactone, 100 μM sodium arsenite, or 5 μg/ml tunicamycin (or equivalent volumes of DMSO or H_2O as controls), with seedlings treated for an additional 16 hours prior to harvesting. Alternatively, seedlings were replenished with medium lacking nitrogen (as described above) and treated for a further 16 hours prior to tissue harvesting, or subjected to a 30 minute heat shock and recovery. Typically, ~100 mg of dry seeds were used per culture, resulting in ~5 g of fresh weight tissue. Frozen tissue was ground to a fine powder, and proteins were extracted with 1.25 volumes of Buffer B (50 mM HEPES (pH 7.5), 50 mM NaCl, 10 mM $MgCl_2$, 10 % (v/v) glycerol, with 10 mM ATP, 5 mM dithiotreithol, 2 mM phenylmethylsulfonyl fluoride and 6 μM chymostatin (Sigma-Aldrich) added immediately before use). Extracts were filtered through two layers of Miracloth (Calbiochem) and clarified at 30,000 × *g* for 20 minutes at 4 °C. The supernatant was immediately applied three times over a 12 ml PolyPrep® chromatography column (Bio-Rad) containing 100 μl (equal to a 50 μl bead volume) of anti-FLAG® M2 affinity resin (Sigma-Aldrich). The column was then washed three times with 2 ml of Buffer B. Where indicated, beads were incubated for 16 hours at 16 °C with the catalytic domain of the deubi-

quitylating enzyme (DUB) USP2 (Boston Biochem, product number E504), at a concentration of 10 nM in a volume of 300 µl. The column was washed three times with 2 ml of Buffer B to remove the DUB and any ubiquitin that had been released. Remaining bound protein was eluted by incubating the beads for 30 minutes at 4 °C with 250 µl of Buffer B containing 500 ng/µl of the FLAG peptide (DYKDDDDK, synthesised by the University of Wisconsin Biotechnology Center Peptide Synthesis Facility). Samples of the crude extract, flow through (both diluted 1/10), third wash step and elution were analyzed by native- or SDS-PAGE, followed by silver staining or immunoblotting with antibodies against various proteasome subunits and ubiquitin.

Native-PAGE was performed essentially as previously described (Elsasser *et al.*, 2005), with minor modifications. Briefly, the resolving gel was composed of 4.5 % acrylamide, 0.12 % bis-acrylamide, 2.3 % sucrose, 1 × TBE (i.e. 89 mM Tris-HCl (pH 8.4), 89 mM H_3BO_3, 2 mM EDTA), 5 mM $MgCl_2$, and 1 mM ATP, whereas the stacking gel was composed of 2.5 % acrylamide and 0.62 % bis-acrylamide, with other components the same as for the resolving gel. Samples containing 10 % glycerol were supplemented with xylene cyanol to 0.0005 %, and gels were run for 18 hours at 4 °C in 1 × TBE supplemented with 0.5 mM ATP, with a constant current of 50 V. Proteins were visualized by staining the gel with silver.

Yeast two-hybrid assays

Assays for protein-protein interactions by yeast two-hybrid were performed using the ProQuest™ Two-Hybrid System (Life Technologies). The indicated genes were amplified by PCR from *Arabidopsis* cDNA generated as described above and recombined into pDONR™221 via the Gateway® BP clonase™ II reaction. The cDNAs were then recombined in-frame to either the GAL4 activation domain or GAL4 binding domain in the pDEST™22 or pDEST™32 vectors (Life Technologies), respectively. Forms of RPN10 containing mutations in one or more of the three ubiquitin-interacting motifs (UIMs) were cloned from previously described constructs in pET42a (Lin *et al.*, 2011), which were provided by Dr. Hongyong Fu (Academia Sinica, Taiwan). Full-length cDNAs from other species were cloned in the same way as *Arabidopsis*, with cDNA from *Brachypodium distachyon* cv. Bd21 being provided by Daniel P. Woods (University of Wisconsin), and from *Zea mays* cv. B73 and *Physcomitrella patens* cv. Gransden 2004 being provided by Robert C. Augustine (University of Wisconsin). Details of all genes cloned are given in Supplemental Table 4.

All constructions were verified as correct by sequencing, and pairwise combinations of genes in pDEST™22 and pDEST™32 (or the empty vectors as controls) were co-transformed into the *Saccharomyces cerevisiae* strain MaV203. Cells transformed with both plasmids were selected by growth for two days at 30 °C on drop-out medium lacking leucine and tryptophan. Protein-protein interactions were then identified by growth for two days at 30 °C on medium lacking leucine, tryptophan and histidine, and containing 25 mM 3-amino-1,2,4-triazole (3-AT), with at least four individual colonies tested for each interaction pair. To confirm the interaction, single colonies were diluted in sterile

water to an OD_{600} of 0.1, and 5 µl was spotted onto both types of selective media and again grown for two days at 30 °C.

Protein purification and *in vitro* binding assays

For protein expression, the indicated genes were cloned into pDONR™221 as described above, and then recombined in-frame with either glutathione S-transferase (GST, for RPN10-based constructs) or 6His tag (for ATG8-based constructs) in the pDEST™15 or pDEST™17 vectors (Life Technologies), respectively. The GST protein alone, encoded in the unmodified pGEX-4T plasmid (GE Healthcare), was used as a control for the GST-RPN10 fusions. All proteins were expressed in *Escherichia coli* strain BL21(DE3) pLysS. The cells were cultured at 37 °C in 800 ml LB media to an OD_{600} of 0.6-0.8, followed by a 4-hour induction with 1 mM isopropyl-β-D-thiogalactopyranoside, also at 37 °C. Cells were harvested by centrifugation at 5,000 × *g* for 20 minutes at 4 °C, frozen in liquid nitrogen, and lysed in two rounds of 10 ml BugBuster® Master Mix (EMD4 Biosciences), as according to the manufacturer's instructions. GST or GST fusion proteins were affinity purified using GST-Bind™ Resin (EMD4 Biosciences), as according to the manufacturer's instructions with some minor modifications (Kim *et al.*, 2013). Briefly, bacterial cell lysate was incubated with 2 ml PBS-washed GST-Bind™ Resin for 1 hour at 4 °C with continual rotation, then applied to a 30 ml EconoPac® chromatography column (Bio-Rad). After allowing 5 minutes for the beads to settle, the flow-through was allowed to run out and beads were washed twice with ice-cold PBS containing 1 M NaCl and once with ice-cold PBS containing 2 M NaCl. Bound proteins were eluted with 10 ml of ice-cold 25 mM MOPS-KOH (pH 7.5) containing 10 mM reduced glutathione (GSH), and the purified proteins were dialyzed overnight at 4 °C against 25 mM MOPS-KOH (pH 7.5), before being concentrated 10-fold using an Amicon® Ultra-15 centrifugal filter unit with a 10 kDa cut-off limit (Millipore).

Proteins tagged with 6His were affinity purified using nickel-nitrilotriacetic acid (Ni-NTA) agarose beads (QIAGEN). Bacterial cell lysates in BugBuster® Master Mix containing 10 mM imidazole were applied three times to 1 ml PBS-washed Ni-NTA beads in a 30 ml EconoPac® chromatography column at 4 °C. After flow-through, the beads were washed once with NaH_2PO_4 wash buffer (50 mM NaH_2PO_4 (pH 7.8), 300 mM NaCl, 20 mM imidazole), once with Tris-40 buffer (50 mM Tris-HCl (pH 7.8), 300 mM NaCl, 40 mM imidazole), and once with Tris-60 buffer (50 mM Tris-HCl (pH 7.8), 300 mM NaCl, 60 mM imidazole). Bound proteins were then eluted with 5 ml ice-cold elution buffer (50 mM Tris-HCl (pH 7.8), 100 mM NaCl, 300 mM imidazole), and purified proteins were dialyzed overnight at 4 °C to remove the imidazole. Ubiquitin chains were purchased from Boston Biochem (product number UC-230).

To test interactions *in vitro*, only the C-terminal portion of RPN10 (amino acids 201-386) and the ATG8e and f isoforms were used, due to the insolubility of recombinant full-length RPN10 tagged with GST, and the ATG8a and ATG8i isoforms tagged with 6His. To test the direct interaction between RPN10 and ATG8, equal amounts (5 µg) of the two potential interactors were combined in 500

µl of binding buffer (150 mM Tris-HCl (pH 7.4), 300 mM NaCl, 5 mM $MgCl_2$, 1 mM DTT, 5 % (v/v) glycerol, 0.01 % (v/v) Triton X-100). Binding was allowed to proceed for 2 hours at 4 °C, before the addition of 100 µl GST-Bind™ Resin, which had been pre-washed with binding buffer. Samples were incubated for a further 2 hours at 4 °C with continual rotation, and beads were then pelleted by centrifugation at 3,000 × *g* for 1 minute at 4 °C. The beads were subsequently washed 5 times with ice-cold binding buffer, and any bound proteins were eluted in 2 × SDS-PAGE sample buffer by heating at 95 °C for 5 minutes. Samples were analyzed by SDS-PAGE followed by immunoblotting with anti-ATG8 or anti-GST antibodies. The three-way pulldown to confirm the simultaneous interaction of RPN10 with both ATG8 and ubiquitin was performed as above with equal amounts (2 µg) of the three interactors, with the exception that the binding buffer contained 150 mM NaCl, and that Ni-NTA agarose beads were used to perform the pulldown.

To quantify the affinity of the RPN10-ATG8 interaction, a quantitative equilibrium binding assay was performed as previously described (Pollard, 2010). Varying concentrations of 6His-ATG8e (from 0 to 40 µM) were incubated with 1 µM GST-RPN10 (201-386) in 100 µl binding buffer. Binding was allowed to proceed for 2 hours at 4 °C, before the addition of 40 µl Ni-NTA beads, which had been pre-washed with binding buffer. Samples were incubated for a further 2 hours at 4 °C with continual rotation, and beads were then pelleted by centrifugation at 3,000 × *g* for 1 minute at 4 °C. The supernatant was removed and 50 µl was analyzed by SDS-PAGE followed by immunoblotting with anti-ATG8 or anti-GST antibodies. The intensity of the RPN10 bands was quantified as above, with the amount remaining in the supernatant when 6His-ATG8e was absent set at 100 % (or 0 % bound). The percentage of RPN10 bound was then plotted against the concentration of 6His-ATG8e, and the K_d was determined by the concentration of 6His-ATG8e at which 50% of the GST-RPN10 (201-386) protein was bound.

Sequence alignment and phylogenetic analysis

The predicted full-length nucleotide and protein sequences for *Arabidopsis thaliana* RPN10 (obtained from the TAIR database at www.arabidopsis.org) were used as queries in BLAST searches for related loci in other plant genomes available in the Joint Genome Initiative's Phytozome database (www.phytozome.net). The positions of the vWA domain and the three UIMs were predicted by the SMART (www.smart.embl-heidelberg.de) and PFAM (www.pfam.sanger.ac.uk) databases. Progressive alignment of the predicted full-length amino acid sequences was performed with Clustal Omega (www.clustal.org/omega) using the default settings (Sievers *et al.*, 2011). Following minor manual editing, the final alignment was displayed with BoxShade version 3.2 (www.ch.embnet.org/software/BOX_form.html).

The previously reported sequences of all ATG8 isoforms from *Arabidopsis* and yeast (Doelling *et al.*, 2002) were aligned as described above. A Bayesian phylogenetic analysis was performed with MrBayes version 3.1 (Ronquist and Huelsenbeck, 2003), using the General Time Reversible evo-

lutionary model with the mixed amino acid model and γ-distributed rate variation with a proportion of invariable sites. The software was run for 1,000,000 generations, with a sampling frequency of 1,000 generations. The first 250,000 generations (25 %) were discarded as "burn-in" after checking that the log likelihood values had plateaued and that the potential scale reduction factor was close to 1.00. The resulting strict consensus tree was subsequently displayed using TreeView (Page, 1996).

Statistical analysis

Quantified immunoblots were statistically analyzed by one-way analysis of variance (ANOVA) to determine the presence of any significant differences, followed by Tukey's post-hoc tests to identify individual significantly different data points.

Accession numbers

All accession number for genes and proteins used in this study are given in Supplemental Table 4.

SUPPLEMENTAL REFERENCES

Alonso, J. M., Stepanova, A. N., Leisse, T. J., Kim, C. J., Chen, H., Shinn, P., Stevenson, D. K., Zimmerman, J., Barajas, P., Cheuk, R., *et al.* (2003). Genome-wide insertional mutagenesis of *Arabidopsis thaliana. Science.* **301,** 653-657.

Babiychuk, E., Fuangthong, M., Van Montagu, M., Inzé, D., and Kushnir, S. (1997). Efficient gene tagging in *Arabidopsis thaliana* using a gene trap approach. *Proc. Natl. Acad. Sci. USA.* **94,** 12722-12727.

Book, A. J., Smalle, J., Lee, K. H., Yang, P., Walker, J. M., Casper, S., Holmes, J. H., Russo, L. A., Buzzinotti, Z. W., Jenik, P. D., and Vierstra, R. D. (2009). The RPN5a subunit of the 26S proteasome is essential for gametogenesis, sporophyte development and complex assembly in *Arabidopsis. Plant Cell.* **21,** 460-478.

Bustin, S. A., Benes, V., Garson, J. A., Hellemans, J., Huggett, J. F., Kubista, M., Mueller, R. D., Nolan, T., Pfaffl, M. W., Shipley, G. L., *et al.* (2009). The MIQE guidelines: minimum information for publication of quantitative real-time PCR experiments. *Clin. Chem.* **55,** 611-622.

Citovsky, V., Lee, L. Y., Vyas, S., Glick, E., Chen, M. H., Vainstein, A., Gafni, Y., Gelvin, S. B., and Tzfira, T. (2006). The subcellular localisation of interacting proteins by bimolecular fluorescence complementation *in planta*. *J. Mol. Biol.* **362,** 1120-1131.

Clough, S. J., and Bent, A. F. (1998). Floral dip: a simplified method for *Agrobacterium*-mediated transformation of *Arabidopsis thaliana*. *Plant J.* **16,** 735-743.

Curtis M. D., and Grossniklaus, U. (2003). A Gateway cloning vector set for high-throughput functional analysis of genes *in planta*. *Plant Physiol.* **133,** 462-469.

Cutler, S. R., Ehrhardt, D. W., Griffiths, J. S., and Somerville, C. R. (2000). Random GFP:: cDNA fusions enable visualisation of sub-cellular structures in cells of *Arabidopsis* at high frequency. *Proc. Natl. Acad. Sci. USA.* **97,** 3718-3723.

Czechowski, T., Stitt, M., Altmann, T., Udvardi, M. K., and Scheible, W. R. (2005). Genome-wide identification and testing of superior reference genes for transcript normalisation is *Arabidopsis. Plant Physiol.* **139,** 5-17.

Doelling, J. H., Walker, J. M., Friedman, E. M., Thompson, A. R., and Vierstra, R. D. (2002). The APG8/12-activating enzyme APG7 is required for proper nutrient recycling and senescence in *Arabidopsis thaliana. J. Biol. Chem.* **277,** 33105-33114.

Earley, K. W., Haag, J., Pontes, O., Opper, K., Juehne, T., Song, K., and Pikaard, C. S. (2006). Gateway-compatible vectors for plant functional genomics and proteomics. *Plant J.* **45,** 616-629.

Elsasser, S., Schmidt, M., and Finley, D. (2005). Characterisation of the proteasome using native gel electrophoresis. *Methods Enzymol.* **398,** 353-363.

Hennegan, K., P., and Danna, K. J. (1998). pBIN20: an improved binary vector for *Agrobacterium*-mediated transformation. *Plant Mol. Biol. Rep.* **16,** 129-131.

Hofius, D., Schultz-Larsen, T., Jönsen, J., Tsitsigiannis, D. I., Petersen, N. H., Mattsson, O., Jørgensen, L. B., Jones, J. D. G., Mundy, J., and Petersen, M. (2009). Autophagic components contribute to hypersensitive cell death in *Arabidopsis*. *Cell.* **137,** 773-783.

Hong, S. W., and Vierling, E. (2001). Hsp101 is necessary for plant heat tolerance but dispensable for development and germination in the absence of stress. *Plant J.* **27,** 25-35.

Karimi, M., Inzé, D., and Depicker, A. (2002). Gateway vectors for *Agrobacterium*-mediated plant transformation. *Trends Plant Sci.* **7,** 193-195.

Kisselev, A. F., and Goldberg, A. L. (2005). Monitoring activity and inhibition of 26S proteasomes with fluorogenic peptide substrates. *Methods Enzymol.* **398,** 364-378.

Kleinboelting, N., Huep. G., Kloetgen, A., Viehoever, P., Weisshaar, B. (2012). GABI-Kat simple search: recent new features of the *Arabidopsis thaliana* T-DNA mutant database. *Nucleic Acids Res.* **40,** 1211-1215.

Li, F., Chung, T., and Vierstra, R. D. (2014). ATG11 plays a critical role in both general autophagy and senescence-induced mitophagy in *Arabidopsis*. *Plant Cell.* **26,** 788-807.

Martin, K. M., Kopperud, K., Chakrabarty, R., Banerjee, R., Brooks, R. E., and Goodin, M. M. (2009). Transient expression in *Nicotiana benthamiana* fluorescent marker lines provides enhanced definition of protein localisation, movement and interactions *in planta*. *Plant J.* **59,** 150-162.

Nelson, B. K., Cai, X., and Nebenführ, A. (2007). A multi-coloured set of *in vivo* organelle markers for co-localisation studies in *Arabidopsis* and other plants. *Plant J.* **51,** 1126-1136.

Ohad, N., Shichrur, K., and Yalovsky, S. (2007). Analysis of protein-protein interactions in plants by bimolecular fluorescence complementation. *Plant Physiol*. **145,** 1090-1099.

Page, R. D. (1996). TreeView: an application to display phylogenetic trees on personal computers. *Comput. Appl. Biosci.* **12,** 357-358.

Pedrazzini, E., Giovinazzo, G., Bielli, A., de Virgilio, M., Frigerio, L., Pesca, M., Faoro, F., Bollini, R., Ceriotti, A., and Vitale, A (1997). Protein quality control along the route to the plant vacuole. *Plant Cell.* **9,** 1869-1880.

Pfaffl, M. W. (2001). A new mathematical model for relative quantification in real-time RT-PCR. *Nucleic Acids Res.* **29,** 45.

Pollard, T. D. (2010). A guide to simple and informative binding assays. *Mol. Biol. Cell.* **21,** 4061-4067.

Rancour, D. M., Dickey, C., Park, S., and Bednarek, S. Y. (2002). Characterisation of AtCDC48: evidence for multiple membrane fusion mechanisms at the plane of cell division in plants. *Plant Physiol.* **130,** 1241-1253.

Remans, T., Keunen, E., Bex, G. J., Smeets, K., Vangronsveld, J., and Cuypers, A. (2014). Reliable gene expression analysis by reverse transcription quantitative PCR: reporting and minimalising the uncertainty in data accuracy. *Plant Cell.* **26,** 3829-3837.

Ronquist, F., and Huelsenbeck, J. P. (2003). Bayesian phylogenetic inference under mixed models. *Bioinformatics*. **19,** 1572-1574.

Sessions, A., Burke, E., Presting, G., Aux, G., McElver, J., Patton, D. H., Dietrich, B., Ho, P., Bacwaden, J., Ko, C., *et al.* (2002). A high-throughput *Arabidopsis* reverse genetics system. *Plant Cell.* **14,** 2985-2994.

Sievers, F., Wilm, A., Dineen, D., Gibson, T. J., Karplus, K., Li, W., Lopez, R., McWilliam, H., Remmert, M., Söding, J., *et al.* (2011). Fast, scalable generation of high-quality protein multiple sequence alignments using Clustal Omega. *Mol. Syst. Biol.* **7,** 539.

Smalle, J., Kurepa, J., Yang, P., Babiychuk, E., Kushnir, S., Durski, A., and Vierstra, R. D. (2002). The cytokinin growth response in *Arabidopsis* involve the 26S proteasome subunit RPN12. *Plant Cell.* **14,** 17-32.

Sparkes, I. A., Runions, J., Kearns, A., and Hawes, C. (2006). The rapid, transient expression of fluorescent fusion proteins in tobacco plants, and generation of stably transformed plants. *Nat. Protoc.* **1,** 2019-2025.

Thompson, A. R., Doelling, J. H., Suttangkakul, A., and Vierstra, R. D. (2005). Autophagic nutrient recycling in *Arabidopsis* directed by the ATG8 and ATG12 conjugation pathways. *Plant Physiol.* **138,** 2097-2110.

Ueda, M., Matsui, K., Ishiguro, S., Sano, R., Wada, T., Paponov, I., Palme, K., and Okada, K. (2004). The *HALTED ROOT* gene encoding the 26S proteasome subunit RPT2a is essential for the maintenance of *Arabidopsis* meristems. *Development.* **131,** 2101-2111.

Yang, P., Fu, H., Walker, J. M., Papa, C. M., Smalle, J., Ju, Y. M., and Vierstra, R. D. (2004). Purification of the *Arabidopsis* 26S proteasome: biochemical and molecular analyses reveal the presence of multiple isoforms. *J. Biol. Chem.* **279,** 6401-6413.

Zhou, J. Wang, J., Cheng, Y., Chi, Y. J., Fan, B., Yu, J. Q., and Chen, Z. (2013). NBR1-mediated selective autophagy targets insoluble ubiquitinated protein aggregates in plant stress responses. *PLoS Genet.* **9,** e1003196.